Organometallics **1999,** *18,* 4845−4855

Reactivity of Naphthylimines toward $Fe_2(CO)_9$: Observation of Three Different Hydrogen Migration Pathways[#]

Wolfgang Imhof*

Institut für Anorganische und Analytische Chemie, August-Bebel-Strasse 2, 07743 Jena, Germany

Received February 2, 1999

The reaction of $Fe_2(CO)_9$ with imine ligands derived from α- or β-naphthylcarbaldehydes leads to the formation of a series of iron carbonyl complexes. Most of them are produced by a C−H activation reaction in ortho position with respect to the exocyclic imine function. The reaction then proceeds via subsequent intramolecular hydrogen shift reactions and leads to several dinuclear compounds. Three different types of these hydrogen-transfer reactions were observed: a 1,3 hydrogen shift toward the former imine carbon atom, a 1,4 hydrogen shift toward the former imine nitrogen atom, or a 1,3 shift reaction toward one of the aromatic carbon atoms of the naphthalene system, which thus leaves the exocyclic imine function unreacted. In the reaction of β-naphthyl derivatives the formation of trinuclear complexes is observed by the η^4-coordination of a third $Fe(CO)_3$ group to the second ring of the naphthalene. Besides this, the first example of a structurally characterized (η^4-1-azadiene)-$Fe(CO)_3$ complex with the C−C double bond formally being part of a cyclic aromatic system is obtained as a byproduct.

Introduction

The understanding of C−H activation processes is one important factor in the development of catalytic C−C bond formation reactions. Due to this fact, both inter- and intramolecular C−H activation reactions have been intensively studied and thoroughly reviewed in the last years.[1] In recent times C−H activation reactions of aromatic imines or ketones have been used to develop catalytic C−C coupling reactions with CO and/or a wide variety of olefins.[2] So we are interested in the reactivity of α,β-unsaturated imines toward metal carbonyls of group 8 metals. The reactivity of imine ligands derived from cinnamaldehyde toward $Ru_3(CO)_{12}$ has been reported to yield a series of di-, tri-, and tetranuclear ruthenium cluster compounds.[3] These cluster compounds are formed by metalation of the ligand at the imine carbon atom or in β-position and in some cases by subsequent hydrogen shift reactions. The reaction of $Ru_3(CO)_{12}$ with imines of benzaldehyde leads to the formation of either mononuclear complexes of the general formula $Ru(imine)_2(CO)_2$ with orthometalated ligands or a trinuclear ruthenium cluster compound in which the imine is only coordinated via its C−N double bond.[4] On the other side, it is well-known that 1-azadiene ligands react with $Fe_2(CO)_9$ to give mononuclear complexes of the type (η^4-azadiene)$Fe(CO)_3$.[5] In contrast α,β-unsaturated imines in which the C−C double bond is part of a heterocyclic or carbocyclic aromatic system react with $Fe_2(CO)_9$ by means of a C−H activation reaction in β-position to the exocyclic imine group.[6] The reaction then proceeds via a 1,3 hydrogen shift reaction to produce a μ_2-η^3-enyl-amido ligand bridging an Fe_2-

---

* Corresponding author. E-mail: cwi@rz.uni-jena.de.

[#] Part of this work has been presented at the XIIth FECHEM Conference on Organometallic Chemistry 1997, Prague, Czech Republic.

[1] (a) Brookhart, M.; Green, M. L. H. *J. Organomet. Chem.* **1983**, *250*, 395−408. (b) Constable, E. C. *Polyhedron* **1984**, *3*, 1037−1057. (c) Halpern, J. *Inorg. Chim. Acta* **1985**, *100*, 41−48. (d) Crabtree, R. H. *Chem. Rev.* **1985**, *85*, 245−269. (e) Ryabov, A. D. *Chem. Rev.* **1990**, *90*, 403−424. (f) Davies, J. A., Ed. *Selective Hydrocarbon Activation*; VCH: Weinheim, 1990. (g) Arndtsen, B. A.; Bergman, R. G.; Mobley, T. A.; Petersen, T. H. *Acc. Chem. Res.* **1995**, *28*, 154−162. (h) Crabtree, R. H. *Chem. Rev.* **1995**, *95*, 987. (i) Fujiwara, Y.; Takagi, K.; Taniguchi, Y. *Synlett* **1996**, 591−599.

[2] (a) Ketones: Sonoda, M.; Kakiuchi, F.; Chatani, N.; Murai, S. *Bull. Chem. Soc. Jpn.* **1997**, *70*, 3117−3128, and literature cited therein. (b) Imines: Kakiuchi, F.; Yamauchi, F.; Chatani, N.; Murai, S. *Chem. Lett.* **1996**, 111−112. (c) Fukuyama, T.; Chatani, N.; Kakiuchi, F.; Murai, S. *J. Org. Chem.* **1997**, *62*, 5647−5650. (d) Fukuyama, T.; Chatani, N.; Tatsumi, J.; Kakiuchi, F.; Murai, S. *J. Am. Chem. Soc.* **1998**, *120*, 11522−11523.

[3] (a) Elsevier, C. J.; Mul, W. P.; Vrieze, K. *Inorg. Chim. Acta* **1992**, *198−200*, 689−703, and literature cited therein. (b) Imhof, W. *J. Chem. Soc., Dalton Trans.* **1996**, 1429−1436. (c) Mul, W. P.; Elsevier, C. J.; Polm, L. H.; Vrieze, K.; Zoutberg, M. C.; Heijdenrijk, D.; Stam, C. H. *Organometallics* **1991**, *10*, 2247−2259.

[4] (a) Bennett, R. L.; Bruce, M. I.; Goodall, B. L.; Iqbal, M. Z.; Stone, F. G. A. *J. Chem. Soc., Dalton Trans.* **1972**, 1787−1791. (b) Basu, A.; Bhaduri, S.; Sharma, K.; Jones, P. G. *J. Chem. Soc., Chem. Commun.* **1987**, 1126−1127.

[5] (a) Otsuka, S.; Yoshida, T.; Nakamura, A. *Inorg. Chem.* **1967**, *6*, 20−25. (b) De Cian, A.; Weiss, R. *Acta Crystallogr.* **1972**, *B28*, 3264−3280. (c) Brodie, A. M.; Johnson, B. F. G.; Josty, P. L.; Lewis, J. *J. Chem. Soc., Dalton Trans.* **1972**, 2031−2035. (d) Semmelhack, M. F.; Cheng, C. H. *J. Organomet. Chem.* **1990**, *393*, 237−241. (e) Knölker, H.-J.; Gonser, P. *Synlett* **1992**, 517−520. (f) Knölker, H.-J.; Gonser, P.; Jones, P. G. *Synlett* **1994**, 405−408. (g) Knölker, H.-J.; Baum, G.; Gonser, P. *Tetrahedron Lett.* **1995**, *36*, 8191−8194. (h) Knölker, H.-J.; Goesmann, H.; Gonser, P. *Tetrahedron Lett.* **1996**, *37*, 6543−6546. (i) Kane-Maguire, L. A. P.; Pyne, S. G.; Siu, A. F. H.; Skelton, B. W. *J. Aust. Chem.* **1996**, *49*, 673−676. (j) Knölker, H.-J.; Baum, G.; Foitzik, N.; Goesmann, H.; Gonser, P.; Jones, P. G.; Röttele, H. *Eur. J. Inorg. Chem.* **1998**, 993−1007. (k) Imhof, W.; Göbel, A.; Braga, D.; De Leonardis, P.; Tedesco, E. *Organometallics* **1999**, *18*, 736.

[6] (a) Imhof, W. *J. Organomet. Chem.* **1997**, *533*, 31−43. (b) Imhof, W. *J. Organomet. Chem.* **1997**, *541*, 109−116. (c) Bagga, M. M.; Flannigan, W. T.; Knox, G. R.; Pauson, P. L.; Preston, F. J.; Reed, R. I. *J. Chem. Soc. C* **1968**, 36−40. (d) Imhof, W.; Göbel, A.; Ohlmann, D.; Flemming, J.; Fritzsche, H. *J. Organomet. Chem.* **1999**, *584*, 33.

10.1021/om990067z CCC: $18.00

(CO)$_6$ moiety. A compound of this type has first been reported in ref 6c, where the reaction of benzylideneaniline with $Fe_2(CO)_9$ has been described. The structure was correctly assigned on the basis of NMR data. The same cluster compound is also available from the reaction of $Fe_3(CO)_{12}$ with benzalazine.[7] Only very recently was the first complex of this type derived from a cinnamaldehyde derivative obtained as a byproduct in the synthesis of the corresponding η^4-azadiene compound.[8] A complex that consists of a μ_2-η^3-enyl-amido moiety bridging a dinuclear transition metal fragment also was observed in the reaction of $[CpCo(C_2H_4)_2]$ with *N*-phenylbenzylideneamine.[9] Related iron compounds of the formula $[(R)N-C(H)-C(H)-Fe(CO)_3-C(O)]Fe(CO)_3$ which show a keto group instead of the methylene group in the above-mentioned compounds have been prepared from the reaction of the carbene cluster $(\mu_2\text{-}CH_2)Fe_2(CO)_8$ with phosphine imides in the presence of CO.[10] Thermally induced rearrangement of those binuclear cluster compounds yields the isomeric clusters $[C(H)-C(H)-N(R)-Fe(CO)_3-C(O)]Fe(CO)_3$.[10]

In this report we describe the synthesis and characterization of a series of iron cluster compounds derived from the reaction of $Fe_2(CO)_9$ with imines of α- and *β*-naphthylcarbaldehydes. The reaction proceeds via C−H activation reactions in ortho position with respect to the exocyclic imine group and subsequent intramolecular hydrogen shift reactions. In this context three different types of hydrogen shift reactions will be described. Up to now the reaction of $Fe_2(CO)_9$ with imines from benzaldehyde or heterocyclic aromatic imine ligands was described to include the 1,3 hydrogen transfer reaction from the aromatic ring toward the imine carbon atom.[6] We also observed two new hydrogen migration pathways, namely, the 1,4 hydrogen shift toward the imine nitrogen atom as well as a 1,3 hydrogen transfer to one of the carbon atoms of the naphthalene system. In addition the reaction of $Fe_2(CO)_9$ with α-naphthylidene-*N*-cyclohexylimine leads to the formation of a tetranuclear cluster compound of the general formula $(ligand)_2Fe_4(CO)_{10}$, which shows the same structural features that have been observed for related ruthenium compounds.[3] The reaction of *β*-naphthylidene-*N*-phenylimine with $Fe_2(CO)_9$ on the other hand as a byproduct yields the first example of a mononuclear $Fe(CO)_3$ complex of an azadiene in which the C−C double bond is part of an aromatic system which could also be structurally characterized.

Scheme 1

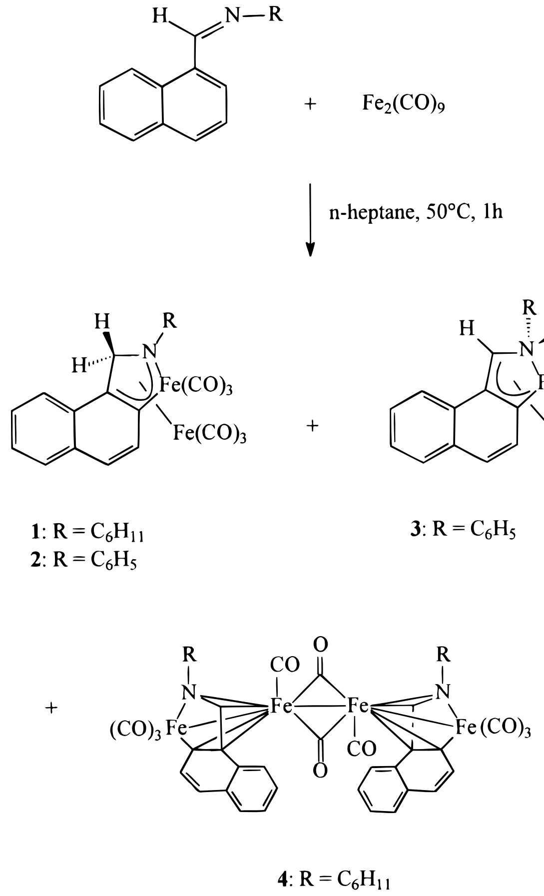

1: R = C_6H_{11}
2: R = C_6H_5
3: R = C_6H_5
4: R = C_6H_{11}

Syntheses of the Compounds

The imine ligands are easily prepared by condensation of the naphthylcarbaldehydes with the corresponding amines adding a catalytic amount of *p*-toluenesulfonic acid. Both imines derived from α-naphthylcarbaldehyde are yellow oils and may be purified by distillation, whereas the ligands from *β*-naphthylcarbaldehyde are solids that may be purified by recrystallization from ethanol.

The reaction of $Fe_2(CO)_9$ with the imines from α-naphthylcarbaldehyde leads to the formation of the iron cluster compounds **1**−**4** (Scheme 1). **1** and **2** are the main products of the reactions, whereas **3** is only formed for R being phenyl and the tetranuclear cluster compound **4** is only produced with cyclohexyl being attached to nitrogen. In all cases a C−H activation in ortho position with respect to the exocyclic imine function is observed. So in a first reaction step an iron hydride species that is stabilized by the nitrogen lone pair of the imine moiety in ortho position may be produced as an intermediate. The formation of **1** and **2** further proceeds by an intramolecular 1,3 hydrogen shift reaction of the hydrogen atom toward the former imine carbon atom, producing a methylene group instead. The formation of **3** may be rationalized by an intramolecular 1,4 hydrogen shift reaction toward the former imine nitrogen atom. In the formation of **4** no hydrogen shift reaction is observed.

The main products of the reaction of *β*-naphthylcarbaldimines with $Fe_2(CO)_9$ (Scheme 2) are the dinuclear cluster compounds **5** and **6**, which show very similar

---

[7] (a) Nametkin, N. S.; Tyurin, V. D.; Trusov, V. V.; Batsanov, A. S.; Struchkov, Y. T. *J. Organomet. Chem.* **1981**, *219*, C26−C28. (b) Nametkin, N. S.; Tyurin, V. D.; Trusov, V. V.; Nekhaev, A. I.; Alexandrov, G. G.; Parpiev, N. A.; Tashev, M. T.; Doustov, H. B. *J. Organomet. Chem.* **1984**, *276*, 199−204. (c) Nametkin, N. S.; Tyurin, V. D.; Trusov, V. V.; Nekhaev, A. I.; Batsanov, A. S.; Struchkov, Y. T. *J. Organomet. Chem.* **1986**, *302*, 243−248.

[8] Knölker, H.-J.; Baum, E.; Gonser, P.; Rohde, G.; Röttele, H. *Organometallics* **1998**, *17*, 3916.

[9] Carofiglio, T.; Stella, S.; Floriani, C.; Chiesi-Villa, A.; Guastini, C. *J. Chem. Soc., Dalton Trans.* **1989**, 1957.

[10] (a) Mirkin, C. A.; Lu, K.-L.; Geoffroy, G. L.; Rheingold, A. L.; Staley, D. L. *J. Am. Chem. Soc.* **1989**, *111*, 7279−7281. (b) Mirkin, C. A.; Lu, K.-L.; Geoffroy, G. L.; Rheingold, A. L. *J. Am. Chem. Soc.* **1990**, *112*, 461−462. (c) Song, J.-S.; Han, S.-H.; Nguyen, S. T.; Geoffroy, G. L.; Rheingold, A. L. *Organometallics* **1990**, *9*, 2386-2395. (d) Mirkin, C. A.; Lu, K.-L.; Snead, T. E.; Young, B. A.; Geoffroy, G. L.; Rheingold, A. L.; Haggerty, B. S. *J. Am. Chem. Soc.* **1991**, *113*, 3800−3810. (e) Snead, T. E.; Mirkin, C. A.; Lu, K.-L.; Nguyen, S.-B. T.; Feng, W.-C.; Beckmann, H. L.; Geoffroy, G. L. *Organometallics* **1992**, *11*, 2613−2622.

Table 1. Bond Lengths [pm] and Angles [deg] of 1 and 2

		1			
Fe1−Fe2	244.7(2)	Fe1−C1	218.0(8)	Fe1−C10	230.2(8)
Fe1−N1	196.8(6)	Fe2−C1	198.8(8)	Fe2−N1	197.5(6)
C1−C10	140(1)	C10−C11	151(1)	C11−N1	146(1)
C1−Fe1−Fe2	50.5(2)	C1−Fe1−C10	36.4(3)	C1−Fe1−N1	74.6(3)
C10−Fe1−Fe2	73.8(2)	C10−Fe1−N1	64.5(3)	N1−Fe1−Fe2	51.8(2)
Fe1−Fe2−C1	57.8(2)	Fe1−Fe2−N1	51.5(2)	Fe1−C1−Fe2	71.7(3)
Fe1−C1−C10	76.5(5)	Fe1−C10−C1	67.1(5)	Fe1−C10−C11	84.5(5)
Fe1−N1−Fe2	76.7(2)	Fe1−N1−C11	99.0(5)	Fe2−C1−C10	113.3(6)
C1−C10−C11	114.3(7)	C10−C11−N1	101.3(6)	C11−N1−Fe2	111.8(5)
		2			
Fe1−Fe2	245.3(1)	Fe1−C1	214.1(4)	Fe1−C10	230.3(4)
Fe1−N1	197.2(3)	Fe2−C1	198.2(4)	Fe2−N1	197.5(3)
C1−C10	140.9(5)	C10−C11	149.8(6)	C11−N1	148.3(5)
C1−Fe1−Fe2	50.6(1)	C1−Fe1−C10	36.8(1)	C1−Fe1−N1	75.0(1)
C10−Fe1−Fe2	74.0(1)	C10−Fe1−N1	65.0(1)	N1−Fe1−Fe2	51.65(9)
Fe1−Fe2−C1	56.5(1)	Fe1−Fe2−N1	51.51(9)	Fe1−C1−Fe2	72.9(1)
Fe1−C1−C10	77.9(2)	Fe1−C10−C1	65.4(2)	Fe1−C10−C11	84.3(2)
Fe1−N1−Fe2	76.8(1)	Fe1−N1−C11	97.7(2)	Fe2−C1−C10	114.3(3)
C1−C10−C11	114.2(4)	C10−C11−N1	101.7(3)	C11−N1−Fe2	111.9(2)

Scheme 2

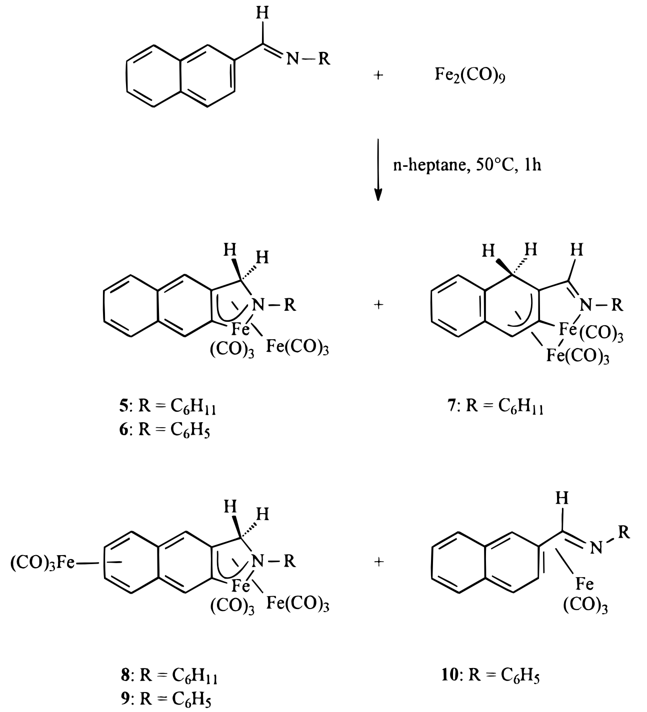

5: R = C_6H_{11}
6: R = C_6H_5
7: R = C_6H_{11}
8: R = C_6H_{11}
9: R = C_6H_5
10: R = C_6H_5

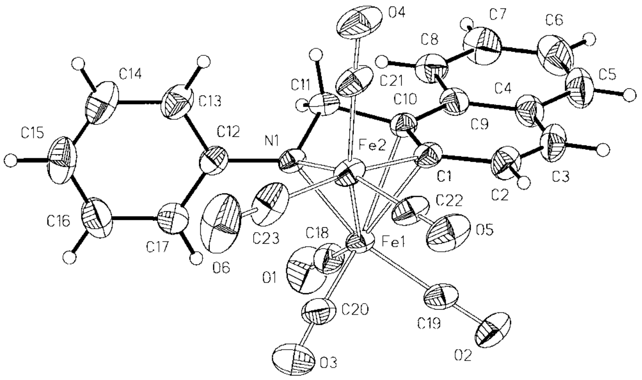

Figure 1. Molecular structure of **2**.

structural features compared to **1** and **2** and which are formed in the same way. **7** is only produced in the reaction with the ligand bearing a cyclohexyl group at the nitrogen atom. In this reaction also an intramolecular 1,3 hydrogen shift reaction takes place, but the hydrogen atom is transferred to the naphthalene system, whereas the imine double bond remains unreacted. The trinuclear iron cluster compounds **8** and **9** are closely related to the compounds **5** and **6** since the C−H activation hydrogen shift reaction sequence at the naphthalene ring bearing the imine substituent proceeds the same way as in the formation of **5** and **6**. In **8** and **9** the second ring of the naphthalene system is η^4-coordinated by an Fe(CO)$_3$ moiety like in the well-known (η^4-butadiene)Fe(CO)$_3$ complexes. In the formation of **5**−**9** the C−H activation reaction always takes place in the 3-position of the naphthalene system. A reaction at the other ortho position has never been observed. The formation of **10** proceeds without a C−H activation reaction but via the η^4-coordination of an Fe(CO)$_3$ moiety to the ligand through the C−N double bond of the imine and the aromatic C−C bond between C$_2$ and C$_3$ of the naphthalene system. This is the first time a η^4-coordination of a α,β-unsaturated imine ligand in which the C−C bond is part of an aromatic system has been structurally characterized.

In all reactions the compounds are separated and purified by chromatography under inert conditions and subsequent recrystallization from mixtures of light petroleum/CH$_2$Cl$_2$ at −20 °C.

Crystal Structure Determinations

Figure 1 shows the molecular structure of **2**; the same numbering scheme has been adopted in the structure analysis of **1**. The most important bond lengths and angles have been summarized in Table 1. In both compounds the naphthalene system has been metalated in ortho position with respect to the exocyclic imine group (C1). The hydrogen atom has been transferred toward the former imine carbon atom (C11). Recently we were able to show this process to proceed via a strictly intramolecular pathway by using selectively deuterated ligands.[6d] The complex thus may also be described as an azaferracyclopentadiene derivative being coordinated to another apical Fe(CO)$_3$ moiety. The bond lengths at C11 are clearly single bonds, as is the metal−metal bond. The only unusual feature is the very

Table 2. Bond Lengths [pm] and Angles [deg] of 3

Fe1−Fe2	258.0(1)	Fe1−C1	211.1(4)	Fe1−C10	209.3(4)
Fe1−C11	204.3(5)	Fe2−C1	198.4(4)	Fe2−N1	206.2(4)
C1−C10	142.0(6)	C10−C11	144.2(6)	C11−N1	146.5(6)
C1−Fe1−Fe2	48.8(1)	C10−Fe1−Fe2	74.3(1)	C11−Fe1−Fe2	71.7(1)
C1−Fe1−C10	39.5(2)	C1−Fe1−C11	68.9(2)	C10−Fe1−C11	40.8(2)
Fe1−Fe2−C1	53.2(1)	Fe1−Fe2−N1	73.3(1)	Fe1−C1−C10	69.6(2)
Fe1−C10−C1	70.9(2)	Fe1−C10−C11	67.8(2)	Fe1−C11−C10	71.5(2)
Fe1−C11−N1	104.7(3)	Fe2−C1−C10	112.5(3)	C1−C10−C11	110.5(4)
C10−C11−N1	114.2(4)	C11−N1−Fe2	100.7(3)	N1−Fe2−C1	83.7(2)

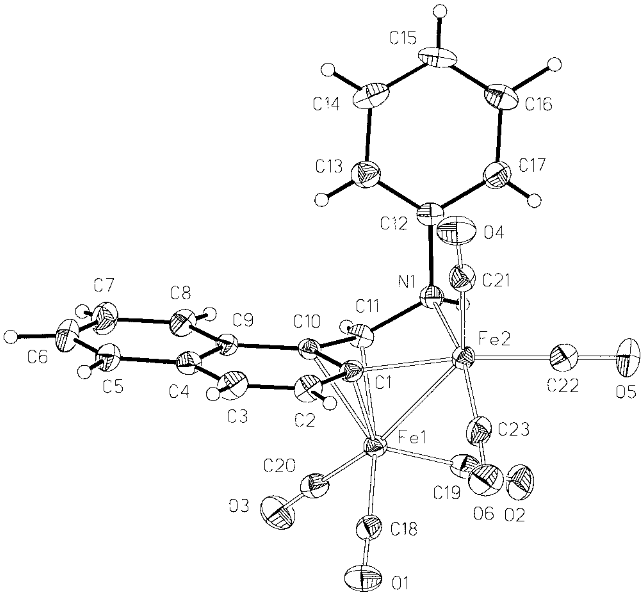

Figure 2. Molecular structure of **3**.

unsymmetrical coordination of Fe1 by C1 and C10, formally the π-coordination of an aromatic double bond. The iron carbon bond length between Fe1 and C1 is about 12 pm (**1**) and 16 pm (**2**), respectively, shorter than the bond between Fe1 and C10. It is very unlikely that this effect is due to steric reasons since it is even stronger for **5** and **6**, as we will see below.

Figure 2 shows the result of the structure analysis of **3**; the most important bond lengths and angles are depicted in Table 2. In **3** the naphthalene system has been metalated at C1, as it has been in the formation of **1** and **2**. But in this case the hydrogen atom has been transferred toward the former imine nitrogen atom, thus forming an amine instead with the nitrogen atom being tetrahedrally surrounded. The lone pair at the amine nitrogen is coordinating to the iron atom which metalated the naphthalene ring (Fe2). The apical $Fe(CO)_3$ group is electronically saturated by a π-allyl coordination toward C1, C10, and C11.

Figure 3 shows the molecular structure of **4**; bond lengths and angles are summarized in Table 3. **4** is a tetranuclear iron complex with the iron atoms building up a chain. Compounds of the same structural type have been shown to be the thermodynamically most stable products in the reaction of $Ru_3(CO)_{12}$ with imine ligands derived from cinnamaldehyde.[3a] Up to now no iron complex of this type has been structurally characterized. Both naphthalene ligands again are metalated by one iron atom in ortho position with respect to the exocyclic imine function. In contrast to the compounds mentioned before, the hydrogen atom being replaced by this metalation reaction is completely removed from the ligand. So the iron atom and the ligand build up a five-membered ring that is absolutely planar and that is coordinated by another apical iron atom, which now is bonded to all atoms of the five-membered ring. The iron atom inside the five-memebered ring shows three terminal CO ligands, whreas the other iron atom is only coordinated by one additional terminal CO ligand. Two of these subunits are linked by a central metal−metal bond that is slightly longer than the other two iron iron bonds as well as two bridging CO groups. Although the molecule in principle shows an internal mirror plane, there is no crystallographic mirror plane since one of the cyclohexyl substituents is disordered.

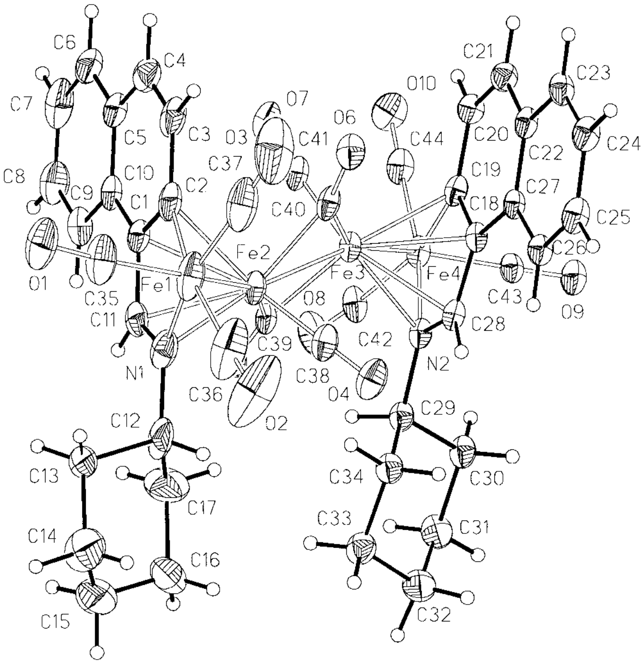

Figure 3. Molecular structure of **4**.

In Figure 4 the molecular structure of **6** is presented; the numbering scheme has been adopted for **5**. The most important bond lengths and angles are summarized in Table 4. In principle **5** and **6** show the same structural features that were already explained for **1** and **2**. The most important difference is the distance between Fe1 and C10, which is 259 pm (**5**) and 268 pm (**6**) and therefore longer than the sum of the covalent radii of iron and carbon. Corresponding to this, the iron−iron bond length in **5** and **6** is about 240 pm on average and thus about 5 pm shorter than was observed for **1** and **2**, respectively. It is also worth noticing that there is selective C−H activation at C1 but never at the second ortho position with respect to the imine function (C9).

Figure 5 shows the result of the structure analysis of **7**; the most important bond lengths and angles are presented in Table 5. The formation of **7** in principle

Table 3. Bond Lengths [pm] and Angles [deg] of 4

Fe1−Fe2	252.1(2)	Fe2−Fe3	258.0(1)	Fe3−Fe4	252.0(1)
Fe1−C2	198(1)	Fe1−N1	195.6(8)	C1−C2	142(1)
C1−C11	144(1)	C11−N1	135(1)	Fe2−C1	222.3(7)
Fe2−C2	223.5(8)	Fe2−C11	212.7(8)	Fe2−N1	207.5(7)
Fe4−C19	198.2(7)	Fe4−N2	195.2(6)	C18−C19	143(1)
C18−C28	141(1)	C28−N2	136.6(8)	Fe3−C18	224.1(6)
Fe3−C19	218.7(7)	Fe3−C28	217.3(7)	Fe3−N2	212.5(5)
Fe1−Fe2−Fe3	154.16(6)	Fe2−Fe3−Fe4	157.48(5)	C2−Fe1−N1	81.4(3)
Fe1−N1−C11	116.2(6)	N1−C11−C1	114.8(8)	C11−C1−C2	113.3(7)
C1−C2−Fe1	113.4(7)	C19−Fe4−N2	81.1(3)	Fe4−N2−C28	116.1(5)
N2−C28−C18	115.1(6)	C28−C18−C19	113.3(6)	C18−C19−Fe4	113.2(5)

Table 4. Bond Lengths [pm] and Angles [deg] of 5 and 6

			5		
Fe1−Fe2	240.52(8)	Fe1−C1	219.2(3)	Fe1−C10	258.6(5)
Fe1−N1	197.9(3)	Fe2−C1	201.3(4)	Fe2−N1	198.1(3)
C1−C10	143.9(5)	C10−C11	149.9(5)	C11−N1	148.9(4)
C1−Fe1−Fe2	51.7(1)	C1−Fe1−C10	33.8(2)	C1−Fe1−N1	74.0(1)
C10−Fe1−Fe2	70.7(2)	C10−Fe1−N1	60.4(2)	N1−Fe1−Fe2	52.62(8)
Fe1−Fe2−C1	58.7(1)	Fe1−Fe2−N1	52.58(8)	Fe1−C1−Fe2	69.6(1)
Fe1−C1−C10	88.3(2)	Fe1−C10−C1	57.9(2)	Fe1−C10−C11	80.3(2)
Fe1−N1−Fe2	74.8(1)	Fe1−N1−C11	104.7(2)	Fe2−C1−C10	112.8(2)
C1−C10−C11	114.0(3)	C10−C11−N1	104.0(3)	C11−N1−Fe2	111.2(2)
			6		
Fe1−Fe2	238.9(2)	Fe1−C1	218.7(7)	Fe1−C10	268(1)
Fe1−N1	198.4(5)	Fe2−C1	205.5(9)	Fe2−N1	197.6(6)
C1−C10	145(1)	C10−C11	149.8(9)	C11−N1	149.9(9)
C1−Fe1−Fe2	53.1(2)	C1−Fe1−C10	32.6(4)	C1−Fe1−N1	73.5(2)
C10−Fe1−Fe2	70.3(4)	C10−Fe1−N1	58.8(4)	N1−Fe1−Fe2	52.7(2)
Fe1−Fe2−C1	58.4(2)	Fe1−Fe2−N1	53.0(2)	Fe1−C1−Fe2	68.5(2)
Fe1−C1−C10	92.8(4)	Fe1−C10−C1	54.6(4)	Fe1−C10−C11	79.1(5)
Fe1−N1−Fe2	74.2(2)	Fe1−N1−C11	107.0(4)	Fe2−C1−C10	112.3(5)
C1−C10−C11	113.8(7)	C10−C11−N1	104.4(5)	C11−N1−Fe2	112.3(4)

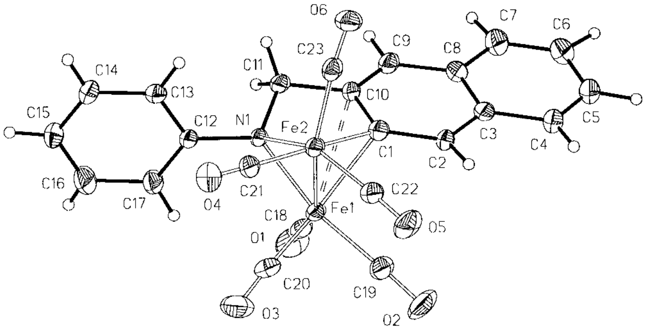

Figure 4. Molecular structure of **6**.

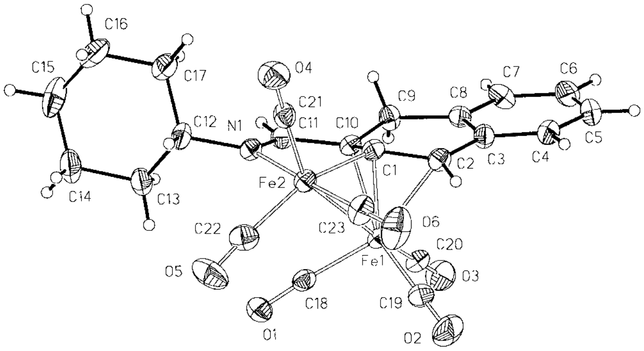

Figure 5. Molecular structure of **7**.

follows a pathway similar to that in the reaction producing **1**, **2**, **3**, **5**, or **6**. Again a C−H activation reaction in ortho position with respect to the imine moiety and a subsequent hydrogen transfer take place, but in this case the hydrogen atom is not transferred to the carbon or nitrogen atom of the imine group but to the second ortho carbon atom of the naphthalene system. So this is the third possibility of a hydrogen migration pathway being observed in the reaction of $Fe_2(CO)_9$ with imines of α- or β-naphthylcarbaldehydes. During the formation of **7** the imine function does not react at all and the carbon−nitrogen bond length still is in the range typical for a double bond. The iron atom bound to C1 is electronically saturated by the coordination to the lone pair at the imine nitrogen atom. The apical iron atom is coordinated in a π-allyl fashion to three carbon atoms of the naphthalene system. The plane of the allyl system is bent out of the plane of the remaining aromatic ring (C3 to C8) by 23°

Figure 6 shows the molecular structure of **9**; the numbering scheme was also adopted for the structure analysis of **8**. The most important bond lengths and angles are depicted in Table 6. The formation of these trinuclear iron complexes is only observed in the reaction of β-naphthylcarbaldimine ligands. The reactivity at the ring bearing the imine group follows the same pathway as in the reaction leading to **5** and **6**. So again the orthometalation 1,3 hydrogen shift reaction sequence is observed leading to the same type of structure that has already been discussed for **5** and **6**. The bond length between Fe1 and C10 in **8** and **9** is about 20 pm shorter than in the corresponding dinuclear complexes **5** and **6**, and corresponding to this observation, the iron−iron distance is about 3 pm longer in **8** and **9**. The third $Fe(CO)_3$ group is η^4-coordinated to the second ring of the naphthalene system, as in the well-known (η^4-butadiene)$Fe(CO)_3$ complexes. As a result of this coordination, the plane of the four carbon atoms being coordinated to the $Fe(CO)_3$ group (C4 to C7) is bent out

Table 5. Bond Lengths [pm] and Angles [deg] of 7

Fe1−Fe2	265.51(5)	Fe1−C1	195.8(2)	Fe1−C2	217.7(2)
Fe1−C10	219.6(2)	Fe2−C1	194.8(2)	Fe2−N1	200.2(2)
C1−C2	141.9(3)	C1−C10	143.2(3)	C10−C11	145.6(3)
C11−N1	127.9(3)	C10−C9	151.0(3)	C9−C8	152.2(3)
C3−C8	140.0(3)	C2−C3	147.4(3)		
Fe2−Fe1−C2	77.47(6)	Fe2−Fe1−C1	47.02(7)	Fe2−Fe1−C10	69.47(6)
C2−Fe1−C1	39.69(9)	C2−Fe1−C10	66.11(8)	C1−Fe1−C10	39.80(9)
Fe1−Fe2−C1	47.35(7)	Fe1−Fe2−N1	88.50(6)	Fe1−C2−C1	61.8(1)
Fe1−C1−C2	78.5(1)	Fe1−C1−C10	79.1(1)	Fe1−C10−C1	61.1(1)
Fe1−C10−C11	111.3(1)	Fe2−C1−C10	110.3(2)	C1−C10−C11	112.3(2)
C10−C11−N1	117.3(2)	C11−N1−Fe2	113.2(2)	N1−Fe2−C1	82.58(8)
C1−C2−C3	121.8(2)	C2−C3−C8	120.6(2)	C3−C8−C9	120.1(2)
C8−C9−C10	113.5(2)	C9−C10−C1	122.7(2)	C10−C1−C2	113.6(2)

Table 6. Bond Lengths [pm] and Angles [deg] of 8 and 9

			8		
Fe1−Fe2	242.34(4)	Fe1−C1	217.3(2)	Fe1−C10	245.4(2)
Fe1−N1	196.9(2)	Fe2−C1	199.8(2)	Fe2−N1	198.3(2)
C1−C10	141.9(3)	C10−C11	149.8(3)	C11−N1	148.0(2)
Fe3−C4	215.7(2)	Fe3−C5	205.7(2)	Fe3−C6	205.9(2)
Fe3−C7	215.7(2)	C3−C4	147.3(3)	C4−C5	142.5(3)
C5−C6	139.8(3)	C6−C7	142.0(3)	C7−C8	147.0(3)
C1−Fe1−Fe2	51.18(5)	C1−Fe1−C10	35.04(7)	C1−Fe1−N1	74.47(6)
C10−Fe1−Fe2	72.08(4)	C10−Fe1−N1	62.16(6)	N1−Fe1−Fe2	52.45(4)
Fe1−Fe2−C1	57.93(5)	Fe1−Fe2−N1	51.93(4)	Fe1−C1−Fe2	70.89(6)
Fe1−C1−C10	83.4(1)	Fe1−C10−C1	61.61(9)	Fe1−C10−C11	82.4(1)
Fe1−N1−Fe2	75.62(5)	Fe1−N1−C11	102.1(1)	Fe2−C1−C10	113.2(1)
C1−C10−C11	115.1(2)	C10−C11−N1	102.4(1)	C11−N1−Fe2	111.7(1)
C4−Fe3−C5	39.44(8)	C4−Fe3−C6	68.99(9)	C4−Fe3−C7	75.59(8)
C5−Fe3−C6	39.71(9)	C5−Fe3−C7	69.20(8)	C6−Fe3−C7	39.28(8)
Fe3−C4−C5	66.5(1)	Fe3−C5−C4	74.0(1)	Fe3−C5−C6	70.2(1)
Fe3−C6−C5	70.1(1)	Fe3−C6−C7	74.1(1)	Fe3−C7−C6	66.6(1)
C3−C4−C5	119.9(2)	C4−C5−C6	115.6(2)	C5−C6−C7	116.3(2)
C6−C7−C8	120.0(2)				
			9		
Fe1−Fe2	242.86(5)	Fe1−C1	218.7(3)	Fe1−C10	244.6(3)
Fe1−N1	197.9(2)	Fe2−C1	201.5(3)	Fe2−N1	199.5(2)
C1−C10	142.2(4)	C10−C11	150.1(4)	C11−N1	148.7(3)
Fe3−C4	214.5(3)	Fe3−C5	205.1(3)	Fe3−C6	204.2(3)
Fe3−C7	216.5(3)	C3−C4	147.5(4)	C4−C5	142.8(4)
C5−C6	141.3(4)	C6−C7	141.9(4)	C7−C8	147.6(4)
C1−Fe1−Fe2	51.45(7)	C1−Fe1−C10	35.19(9)	C1−Fe1−N1	74.52(9)
C10−Fe1−Fe2	72.75(6)	C10−Fe1−N1	62.48(9)	N1−Fe1−Fe2	52.63(6)
Fe1−Fe2−C1	58.08(7)	Fe1−Fe2−N1	52.02(6)	Fe1−C1−Fe2	70.47(8)
Fe1−C1−C10	82.4(2)	Fe1−C10−C1	62.4(1)	Fe1−C10−C11	82.8(2)
Fe1−N1−Fe2	75.35(7)	Fe1−N1−C11	101.6(2)	Fe2−C1−C10	113.4(2)
C1−C10−C11	115.1(2)	C10−C11−N1	102.4(2)	C11−N1−Fe2	112.0(2)
C4−Fe3−C5	39.7(1)	C4−Fe3−C6	70.1(1)	C4−Fe3−C7	76.2(1)
C5−Fe3−C6	40.4(1)	C5−Fe3−C7	69.5(1)	C6−Fe3−C7	39.3(1)
Fe3−C4−C5	66.6(2)	Fe3−C5−C4	73.7(2)	Fe3−C5−C6	69.5(2)
Fe3−C6−C5	70.1(2)	Fe3−C6−C7	75.1(2)	Fe3−C7−C6	65.6(2)
C3−C4−C5	119.2(2)	C4−C5−C6	115.7(3)	C5−C6−C7	116.2(3)
C6−C7−C8	119.2(2)				

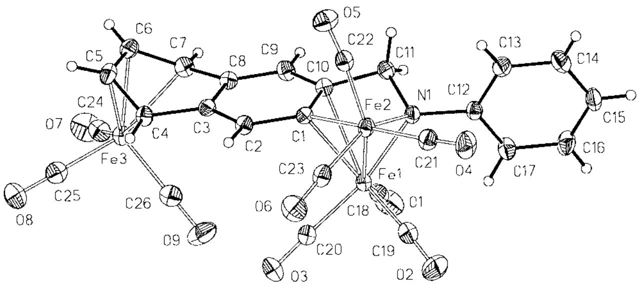

Figure 6. Molecular structure of **9**.

of the plane of the other naphthalene carbon atoms (C1, C2, C3, C8, C9, C10) by 28° (**8**) or 34° (**9**), respectively. There are only a few structurally characterized compounds in which an aromatic π-system is η^4-coordinated to an $Fe(CO)_3$ group including naphthalene and indene derivatives.[11] There is only one example of a benzene derivative described, namely, the $Fe(CO)_3$ complex of 1,2,3,4-tetramethyl-5,6-bis(trifluoromethyl)benzene, which was formed by photolysis of $(\eta^4\text{-}C_4Me_4)Fe(CO)_3$ in the presence of hexafluorobutyne.[12] All other compounds that were published before are very electron poor aromatic compounds such as derivatives of 1,4-diboranaphthalene or 9,10-diboraanthracene.[13]

---

[11] (a) Herbstein, F. H.; Reisner, M. G. *Acta Crystallogr., Sect. B* **1977**, *33*, 3304−3317. (b) Schaufele, H.; Hu, D.; Pritzkow, H.; Zenneck, U. *Organometallics* **1989**, *8*, 396−401. (c) Brodt, C.; Niu, S.; Pritzkow, H.; Stephan, M.; Zenneck, U. *J. Organomet. Chem.* **1993**, *459*, 283−291. (d) Petrel, T. A.; Stephan, J. M.; McDaniel, K. F.; McMills, M. C.; Rheingold, A. L.; Yap, G. P. A. *J. Org. Chem.* **1996**, *61*, 4188−4189. (e) Bennett, M. A.; Lu, Z.; Wang, X.; Bown, M.; Hockless, D. C. R. *J. Am. Chem. Soc.* **1998**, *120*, 10409.

[12] Bond, A.; Bottrill, M.; Green, M.; Welch, A. J. *J. Chem. Soc., Dalton Trans.* **1977**, 2372−2381.

Table 7. Bond Lengths [pm] and Angles [deg] of 10

Fe1−C1	217.6(2)	Fe1−C2	212.4(2)	Fe1−C11	208.8(2)
Fe1−N1	206.2(2)	C1−C2	143.8(3)	C2−C11	142.6(3)
C11−N1	135.5(3)				
C1−Fe1−C2	39.05(9)	C1−Fe1−C11	69.61(9)	C1−Fe1−N1	77.79(8)
C2−Fe1−C11	39.55(9)	C2−Fe1−N1	68.56(8)	C11−Fe1−N1	38.10(8)
Fe1−C1−C2	68.5(1)	Fe1−C2−C1	72.4(1)	Fe1−C2−C11	68.9(1)
Fe1−C11−C2	71.6(1)	Fe1−C11−N1	69.9(1)	Fe1−N1−C11	72.0(1)
C1−C2−C11	116.5(2)	C2−C11−N1	116.0(2)		

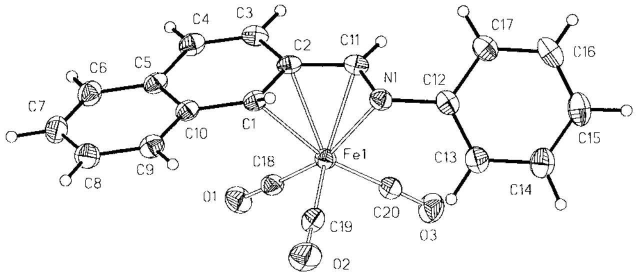

Figure 7. Molecular structure of **10**.

Figure 7 presents the molecular structure of **10**; the most important bond lengths and angles are shown in Table 7. **10** is the first example of a (η^4-azadiene)Fe(CO)$_3$ complex in which the C−C double bond is part of an aromatic system. Up to now only azadiene complexes with ligands derived from acyclic α,β-unsaturated aldehydes have been published.[5] The coordination of the iron atom is slightly unsymmetrical. The bond lengths of iron to the imine nitrogen and the imine carbon atom are of about the same value, whereas the two iron−carbon bond lengths to the naphthalene double bond are significantly longer. The C−C and C−N double bonds of the azadiene are elongated by coordination to the metal, and the central C−C bond is shortened, as was shown to be typical for complexes of this type.[5] Recently we were able to show by means of extended Hückel calculations on (η^4-azadiene)Fe(CO)$_3$ complexes that these compounds stabilize themselves by bending of the hydrogen at the C-terminus of the azadiene chain (C1 in **10**) out of the plane of the azadiene system itself. By this process the overlap of the MOs at C1 and Fe1 is increased.[5k] The same observation can be made in the molecular structure of **10** since the distance of H1 with respect to the plane through N1, C11, C2, and C2 is 54.2 pm.

NMR Spectroscopy

The NMR spectra of **1** and **2** as expected show properties closely related to those of other dinuclear iron complexes derived from imines of monocyclic aromatic ligands.[6] So the most significant feature is the resonances representing the methylene group that is formed during the reaction and is observed at $\delta = 4.20$ (**1**) or $\delta = 4.68$ (**2**), respectively, in the hydrogen NMR and at about $\delta = 74$ for both compounds in the carbon NMR spectra. The signals of the coordinated naphthalene system are also very similar to those reported for benzaldimine complexes (see Experimental Part).[6d] The ^{1}H NMR spectrum of **3** beneath the naphthalene protons shows the NH group at $\delta = 5.26$ and the hydrogen at the former imine carbon atom at $\delta = 4.20$, which is now part of a π-allyl system and is thus shifted to higher field by coordination to the iron atom. This allyl moiety also gives rise to characteristic signals in the ^{13}C NMR spectrum, $\delta = 61.9$, 68.5, and 100.6, whereas the other carbon atoms are observed at expected chemical shifts. The spectroscopical properties of **4** are identical with those of the corresponding ruthenium complexes. NMR measurements at 70 °C in toluene-d_8 have shown that there is no thermally induced interconversion of the isomeric compounds **2** and **3** into each other.

The ^{1}H NMR spectra of **5** and **6** also show the signals representing the methylene groups at $\delta = 4.30$ (**5**) and 4.66 (**6**), respectively, as one characteristic feature. Besides this, the hydrogen atoms at C2 (see Figure 4) are shifted to lower field and give rise to singlets at $\delta = 8.74$ (**5**) and 8.72 (**6**). The corresponding carbon resonances of the methylene group both are observed at $\delta = 76.0$, whereas the signals of the naphthalene system, the organic substituents at nitrogen, and the CO ligands show signals in the expected regions. The NMR spectra of **7** also show characteristic resonances for the methylene group, which in this case was formed at C9 (see Figure 5). The two hydrogen atoms at C9 are diastereotopic and thus give rise to a AB pattern of the signals with a coupling constant of 21.3 Hz. The proton at C2, which is part of a π-allyl system, is observed as a singlet at $\delta = 5.90$, as is the resonance representing the unreacted imine hydrogen at $\delta = 8.17$. The other hydrogen atoms show signals at expected values. In the ^{13}C NMR spectrum of **7** the methylene group occurs in the range of about $\delta = 30$; the carbon atoms of the allyl system show signals at about $\delta = 80$ for the two outer carbon atoms and in the aromatic region for the central carbon atom. The resonance of the imine carbon atom at $\delta = 179.0$ is observed at a 20 pm lower shift compared to the free ligand. The molecular structure of **8** and **9** is closely related to the structures of **5** and **6** (see Figures 4 and 6). In **8** and **9** the same C−H activation hydrogen shift reaction sequence has taken place ortho to the imine function of the free ligand. The second ring of the naphthalene system is coordinating another Fe(CO)$_3$ moiety. The introduction of this third Fe(CO)$_3$ group in **8** and **9** in contrast to the spectra of **5** and **6** now leads to the observation of diastereotopicity at the methylene group (C11, Figure 6). Since it is not reasonable that the Fe$_2$(CO)$_6$ moiety is affected by the new Fe(CO)$_3$ group concerning its fluxionality the reason for the protons at C11 to become diastereotopic must be the bending of the naphthalene system. So the methylene groups in **8** and **9** show an AB spin pattern with a coupling constant of about 12 Hz. The two remaining hydrogen atoms at the first ring of the naphthalene system at C2 and C9 (see Figure 6) give rise to singlets at $\delta = 6.58$ and 7.21, respectively, for **8**. In the NMR

---

(13) (a) Schulz, H.; Pritzkow, H.; Siebert, W. *Chem. Ber.* **1991**, *124*, 2203−2207. (b) Schulz, H.; Pritzkow, H.; Siebert, W. *Chem. Ber.* **1992**, *125*, 987−991.

Table 8. Crystal and Intensity Data for the Compounds 1−4

	1	2	3	4
formula	$C_{23}H_{19}NO_6Fe_2$	$C_{23}H_{13}NO_6Fe_2$	$C_{23}H_{13}NO_6Fe_2$	$C_{44}H_{34}N_2O_{10}Fe_4$
mol weight [g mol^{-1}]	517.09	511.04	511.04	1021.21
radiation	Mo Kα	Mo Kα	Mo Kα	Mo Kα
monochromator	graphite	graphite	graphite	graphite
temperature [K]	213	293	213	183
crystal color	red	red	orange	red-brown
crystal size	0.2 × 0.2 × 0.03	0.4 × 0.3 × 0.1	0.2 × 0.2 × 0.1	0.4 × 0.3 × 0.3
a [Å]	17.261(3)	12.143(3)	10.245(3)	10.6109(7)
b [Å]	8.335(2)	12.981(4)	13.757(3)	13.8439(9)
c [Å]	15.213(2)	16.142(5)	14.906(3)	17.298(1)
α [deg]	90	113.10(1)	92.88(1)	97.284(5)
β [deg]	90	106.20(2)	91.86(2)	102.698(4)
γ [deg]	90	95.20(2)	91.00(1)	90.181(5)
volume [Å^3]	2188.7(7)	2189(1)	2096.7(9)	2457.5(3)
Z	4	4	4	2
F(000)	1056	1032	1032	1044
ρ_{calc} [g cm^{-3}]	1.569	1.551	1.619	1.380
crystal system	orthorhombic	triclinic	triclinic	triclinic
space group	$Pca2_1$	$P\bar{1}$	$P\bar{1}$	$P\bar{1}$
abs coeff [mm^{-1}]	1.365	1.364	1.428	1.212
θ limit	2.36−27.99	1.46−30.64	1.37−36.47	2.43−23.31
scan mode	$\theta-2\theta$	$\theta-2\theta$	$\theta-2\theta$	φ
scan speed [deg min^{-1}]	3−60	3−60	3−60	
no. of reflns measd	3455	9087	7412	6520
no. of indep reflns	2876	8312	6972	6520
R(int)	0.0505	0.0193	0.0349	0.0000
no. of obs reflns $F_o^2 > 2\sigma(F_o^2)$	2041	5717	4979	5162
no. of params	300	597	681	629
GOOF	1.039	0.967	1.017	1.154
R1	0.0575	0.0471	0.0464	0.0738
wR2	0.1079	0.1123	0.0972	0.1585
final diff map electron density [e Å^{-3}]	0.564	0.567	0.449	1.142

spectrum of **9** only the singlet at $\delta = 6.69$ representing the proton at C9 can be identified since the resonance of the hydrogen atom at C2 is overlapped by the multiplet structure of the nitrogen-bound phenyl group. The hydrogen atoms at the second ring of the naphthalene system which is now η^4-coordinated to the third $Fe(CO)_3$ moiety are shifted to higher field compared to the free ligand. Since this "butadiene" subunit is unsymmetrically substituted at the outer carbon atoms, all four hydrogen atoms are different. The inner hydrogen atoms at C5 and C6 (see Figure 6) show a nearly identical chemical shift and thus give rise to multiplet structures in the hydrogen NMR spectra of both **8** and **9** at about $\delta = 6.3$. The signals for the hydrogen atoms at C4 and C7 each show well-separated doublets of doublets at about $\delta = 3.5-3.6$. In the ^{13}C NMR spectra of **8** and **9** the signals of the methylene groups are observed at $\delta = 74.0$ (**8**) and 76. 4 (**9**), respectively. Most typical for these compounds are the resonances of the four carbon atoms coordinated to the third $Fe(CO)_3$ group. For the outer carbon atoms (C4 and C7, see Figure 6) two signals at about $\delta = 62$ are observed for both **8** and **9**, whereas the inner carbon atoms of this "butadiene" subunit give rise to two singlets at $\delta = 67$.

In the NMR spectra of **10** the hydrogen and carbon resonances of the "azadiene" subunit coordinating the $Fe(CO)_3$ group as expected are shifted to higher field compared to the spectra of the free ligand. Their chemical shifts correspond very well with those of the related (η^4-azadiene)$Fe(CO)_3$ complexes with ligands of the cinnamaldehyde type.[5]

Experimental Part

General Procedures. All procedures were carried out under an argon atmosphere in anhydrous, freshly distilled solvents. Chromatography was done using silica gel 60 and silanized silica gel 60, 70-230 mesh ASTM (Merck), which were dried at 10^{-2} bar (10^3 Pa) for 2 days before use. $Fe_2(CO)_9$ was prepared from $Fe(CO)_5$ (Aldrich) by irradiation in acetic acid.[14] Infrared spectra were recorded on a Perkin-Elmer FT-IR System 2000 using 0.2 mm KBr cuvettes. NMR spectra were recorded on a Bruker AC 200 spectrometer (^1H, 200 MHz with $SiMe_4$ as internal standard; ^{13}C, 50.32 MHz with $CDCl_3$ as internal standard); ^1H, ^{13}C, and HMQC spectra of **9** and **10** on a Bruker DRX 400 spectrometer (^1H, 400 MHz; ^{13}C, 100.62 MHz with $CDCl_3$ as internal standard). Mass spectra were recorded on a Finnigan MAT SSQ 710 instrument. Elemental analyses were carried out at the laboratory of the Institute of Organic Chemistry and Macromolecular Chemistry of the Friedrich-Schiller-University Jena.

X-ray Crystallographic Studies. Structure determinations of **1**, **2**, **3**, **5**, and **6** were carried out on a Siemens P4 diffractometer. Structure determinations of **4**, **7**, **8**, **9**, and **10** were carried out using a Enraf Nonius Kappa CCD diffractometer, crystal detector distance 25 mm, 180 frames. In both cases graphite-monochromated Mo Kα radiation was used. The crystals were mounted in a stream of cold nitrogen. Data were corrected for Lorentz and polarization effects but not for absorption. The structures were solved by direct methods and refined by full-matrix least-squares techniques against F^2 using the programs SHELXS86 and SHELXL93.[15] Computations of the structures were done with the program XPMA,[16] and the molecular illustrations were drawn using the program XP.[17] The crystal and intensity data are given in Tables 8 and 9. Additional material on the structure analyses is available from the Cambridge Crystallographic Data Centre by mentioning the deposition numbers 117389 (**1**), 117390 (**2**), 117391

---

[14] Brauer, G. *Handbuch der Präp. Anorg. Chemie*, 8th ed.; VCH: Weinheim, 1968; Part C, No. 1, p 19.

[15] (a) Sheldrick, G. *SHELXS-86*; Universität Göttingen, 1986. (b) Sheldrick, G. *SHELXL-93*; Universität Göttingen, 1993.

[16] Zsolnai, L.; Huttner, G. *XPMA*; Universität Heidelberg, 1996.

[17] *XP−Interactive Molecular Graphics*, Vers. 4.2; Siemens Analytical Xray Inst. Inc., 1990.

Table 9. Crystal and Intensity Data for the Compounds 5−10

	5	**6**	**7**	**8**	**9**	**10**
formula	$C_{23}H_{19}NO_6Fe_2$	$C_{23}H_{13}NO_6Fe_2$	$C_{23}H_{19}NO_6Fe_2$	$C_{26}H_{19}NO_9Fe_3$	$C_{26}H_{13}NO_9Fe_3$	$C_{20}H_{13}NO_3Fe$
mol weight [g mol^{-1}]	517.09	511.04	517.09	656.97	650.92	371.16
radiation	Mo Kα	Mo Kα	Mo Kα	Mo Kα	Mo Kα	Mo Kα
monochromator	graphite	graphite	graphite	graphite	graphite	graphite
temperature [K]	293	213	183	183	183	183
crystal color	purple	purple	red	orange	orange	orange
crystal size	0.2 × 0.2 × 0.2	0.4 × 0.2 × 0.02	0.2 × 0.2 × 0.2	0.3 × 0.2 × 0.05	0.2 × 0.2 × 0.08	0.8 × 0.3 × 0.1
a [Å]	8.779(1)	7.964(5)	8.1509(4)	12.8617(4)	8.2177(4)	11.283(2)
b [Å]	24.927(2)	10.472(2)	10.2714(5)	14.8351(5)	10.7951(5)	16.930(3)
c [Å]	10.046(2)	13.658(3)	13.6492(6)	14.4385(4)	14.7951(5)	9.323(2)
α [deg]	90	75.18(1)	80.111(3)	90	80.207(3)	90
β [deg]	92.93(1)	74.68(3)	89.565(3)	108.781(2)	77.630(3)	110.37(3)
γ [deg]	90	82.65(3)	77.561(3)	90	80.602(2)	90
volume [Å^3]	2195.5(5)	1059.8(7)	1098.88(9)	2608.2(1)	1252.32(9)	1669.5(6)
Z	4	2	2	4	2	4
F(000)	1056	516	528	1328	652	760
ρ_{calc} [g cm^{-3}]	1.564	1.601	1.563	1.673	1.726	1.477
crystal system	monoclinic	triclinic	triclinic	monoclinic	triclinic	monoclinic
space group	$P2_1/n$	$P\bar{1}$	$P\bar{1}$	$P2_1/n$	$P\bar{1}$	$P2_1/c$
abs coeff [mm^{-1}]	1.361	1.409	1.360	1.701	1.771	0.921
θ limit	1.63−27.00	1.59−26.67	3.01−23.26	3.12−23.28	2.68−23.30	2.73−23.27
scan mode	θ-2θ	θ-2θ	φ	φ	φ	φ
scan speed [deg min^{-1}]	3−60	3−60				
no. of reflns measd	5997	5136	2974	6910	3366	4379
no. of indep reflns	4796	4166	2974	3737	3366	2377
R(int)	0.0423	0.0438	0.0000	0.0225	0.0000	0.0439
no. of obs reflns $F_o^2 > 2\sigma(F_o^2)$	3028	2515	2682	3499	3174	2198
no. of params	365	339	369	428	404	278
GOOF	1.023	1.016	1.026	1.017	1.091	1.041
R1	0.0454	0.0622	0.0309	0.0224	0.0260	0.0343
wR2	0.0801	0.1439	0.0690	0.0698	0.0929	0.0892
final diff map electron density [e Å^{-3}]	0.295	0.897	0.250	0.272	0.358	0.300

(**3**), 117392 (**4**), 117393 (**5**), 117394 (**6**), 117395 (**7**), 117396 (**8**), 117397 (**9**), 117398 (**10**), the author, and the journal citation.

Preparation of the Imine Ligands. The imines are prepared by reacting 2 g (12.8 mmol) of α- or β-naphthylcarbaldehyde with an equimolar amount of the corresponding amine (1.27 g cyclohexylamine, 1.19 g aniline). The reaction is carried out in 20 mL of ethanol together with a catalytic amount of p-toluenesulfonic acid and monitored by GC. After the reaction is completed the imines from α-naphthylcarbaldehyde are distilled to yield yellow oily products (R = C_6H_{11}: bp 127 °C, 5.2 × 10^{-5} Torr, yield 2.82 g, 93%. R = C_6H_5: bp 132 °C, 2.9 × 10^{-5} Torr, yield 2.59 g, 86%), whereas the imines from β-naphthylcarbaldehyde crystallize during the reaction. The crude products are collected and recrystallized from ethanol (R = C_6H_{11}: mp 120 °C, yield 2.67 g, 88%. R = C_6H_5: mp 92 °C, yield 1.95 g, 65%).

α-Naphthylidene-*N*-cyclohexylimine: MS (EI) m/z (%) 237 (M^+, 100), 208 ($C_{15}H_{14}N^+$, 18), 194 ($C_{14}H_{12}N^+$, 47), 180 ($C_{13}H_{10}N^+$, 28), 166 ($C_{12}H_8N^+$, 18), 154 ($C_{11}H_8N^+$, 92), 141 ($C_{10}H_7N^+$, 21), 127 ($C_9H_5N^+$, $C_{10}H_7^+$, 26), 83 ($C_6H_{11}^+$, 10), 55 ($C_4H_7^+$, 17), 41 ($C_3H_5^+$, 15); ^{1}H NMR (in $CDCl_3$, 298 K) [ppm] 1.13−1.81 (m, 10H, CH_2), 3.23−3.37 (m, 1H, CH), 7.45−7.60 (m, 3H, CH), 7.80−8.02 (m, 3H, CH), 8.87 (d, $^3J_{HH}$ = 8.38 Hz, 1H, CH), 8.97 (s, 1H, N=CH); ^{13}C NMR (in $CDCl_3$, 298 K) [ppm] 24.8 (CH_2), 25.8 (CH_2), 34.6 (CH_2), 70.8 (CH), 124.4 (CH), 125.2 (CH), 125.9 (CH), 126.9 (CH), 128.3 (CH), 128.5 (CH), 130.5 (CH), 131.4 (C), 132.2 (C), 133.9 (C), 157.9 (CH).

α-Naphthylidene-*N*-phenylimine: MS (EI) m/z (%) 231 (M^+, 70), 230 ($M^+ - H$, 100), 202 ($C_{15}H_8N^+$, 5), 154 ($C_{11}H_8N^+$, 5), 127 ($C_9H_5N^+$, 24), 114 ($C_8H_4N^+$, 8), 101 ($C_7H_3N^+$, 4), 77 ($C_6H_5^+$, 29), 63 ($C_5H_3^+$, 3), 51 ($C_4H_3^+$, 10); ^{1}H NMR ($CDCl_3$, 298 K) [ppm] 7.24−8.27 (m, 11H, CH), 9.13−9.19 (m, 2H, CH, N=CH); ^{13}C NMR ($CDCl_3$, 298 K), [ppm] 120.8 (CH), 124.2 (CH), 125.1 (CH), 125.8 (CH), 126.0 (CH), 127.3 (CH), 128.6 (CH), 129.1 (CH), 129.8 (CH), 131.3 (C), 131.7 (CH, C), 133.7 (C), 152.5 (C), 159.8 (N=CH).

***β*-Naphthylidene-*N*-cyclohexylimine**: MS (EI) m/z (%) 237 (M^+, 91), 208 ($C_{15}H_{14}N^+$, 50), 194 ($C_{14}H_{12}N^+$, 78), 180 ($C_{13}H_{10}N^+$, 39), 167 ($C_{12}H_9N^+$, 23), 154 ($C_{11}H_8N^+$, 100), 139 ($C_{10}H_5N^+$, 41), 127 ($C_9H_5N^+$, $C_{10}H_7^+$, 42), 83 ($C_6H_{11}^+$, 18), 55 ($C_4H_7^+$, 29), 41 ($C_3H_5^+$, 25); ^{1}H NMR ($CDCl_3$, 298 K) [ppm] 1.25−1.90 (m, 11H, CH_2), 3.22−3.32 (m, 1H, CH), 7.47−7.52 (m, 2H, CH), 7.81−8.09 (m, 3H, CH), 8.42 (s, 1H, N=CH); ^{13}C NMR ($CDCl_3$, 298 K) [ppm] 24.7 (CH_2), 25.6 (CH_2), 34.3 (CH_2), 69.7 (CH), 124.0 (CH), 126.1 (CH), 126.7 (CH), 127.6 (CH), 128.1 (CH), 128.3 (CH), 129.3 (CH), 133.0 (C), 134.2 (C), 134.4 (C), 158.3 (N=CH).

***β*-Naphthylidene-*N*-phenylimine**: MS (EI) m/z (%) 231 (M^+, 100), 230 ($M^+ - H$, 86), 202 ($C_{15}H_8N^+$, 7), 153 ($C_{11}H_7N^+$, 3), 139 ($C_{10}H_5N^+$, 7), 127 ($C_9H_5N^+$, 22), 115 ($C_8H_5N^+$, 24), 101 ($C_7H_3N^+$, 8), 89 ($C_7H_5^+$, 3), 77 ($C_6H_5^+$, 62), 63 ($C_5H_3^+$, 3), 51 ($C_4H_3^+$, 15); ^{1}H NMR ($CDCl_3$, 298 K) [ppm] 7.24−7.60 (m, 7H, CH), 7.86−7.95 (m, 3H, CH), 8.18−8.22 (m, 2H, CH), 8.61 (s, 1H, N=CH); ^{13}C NMR ($CDCl_3$, 298 K) [ppm] 120.7 (CH), 123.7 (CH), 125.7 (CH), 126.4 (CH), 127.3 (CH), 127.7 (CH), 128.4 (CH), 128.5 (CH), 128.9 (CH), 130.9 (CH), 132.9 (C), 133.8 (C), 134.8 (C), 151.9 (C), 160.0 (N=CH).

Treatment of α-Naphthylcarbaldimines with $Fe_2(CO)_9$. A 500 mg sample of $Fe_2(CO)_9$ (1.37 mmol) is reacted with 1.64 mmol of the respective α-naphthylcarbaldimine (R = C_6H_{11}, 380 mg; R = C_6H_5, 370 mg) in 30 mL of n-heptane at 50 °C. After 45 min all of the starting material is dissolved and the color of the solution has changed from light yellow to deep red. The volatile material is evaporated in vacuo, and the oily residue is dissolved in 10 mL of CH_2Cl_2. A 2 g portion of silanized silica gel is added, and the solvent is removed in vacuo. The product mixture is chromatographed on silica gel using mixtures of light petroleum (bp 40−60 °C) and CH_2Cl_2. In both reactions at first a small amount of $Fe_3(CO)_{12}$ is eluted. In the reaction of the α-naphthylcarbaldimine with R = C_6H_{11} 392 mg (54.7%) of **1** is obtained using a mixture of light petroleum/CH_2Cl_2 (6:1), and with a mixture of light petroleum/CH_2Cl_2 (1:1) 65 mg (5%) of **4** is observed. Using the α-naphthylcarbaldimine with R = C_6H_5 210 mg (30%) of **2** is obtained with a mixture of light petroleum/CH_2Cl_2 (20:1), and increasing the ratio to 2:1 164 mg (23%) of **3** is collected. **1** and **2** are intensively red colored, whereas **3** is orange and **4** shows a red-brown color. **1**, **2**, and **3** are recrystallized from mixtures of light petroleum/CH_2Cl_2 at −20 °C. **4** is recrystallized from light petroleum/toluene (3:1) at −20 °C.

MS and Spectroscopical Data of 1: MS (EI) *m/z* (%) 517 (M^+, 7), 489 ($M^+ - CO$, 4), 461 ($M^+ - 2$ CO, 16), 433 ($M^+ - 3$ CO, 7), 405 ($M^+ - 4$ CO, 13), 377 ($M^+ - 5$ CO, 63), 349 ($M^+ - 6$ CO, 62), 287 ($C_{17}H_{13}NFe^+$, 19), 266 ($C_{15}H_{16}NFe^+$, 18), 240 ($C_{13}H_{14}NFe^+$, 21), 211 ($C_{15}H_{17}N^+$, 25), 198 ($C_{14}H_{16}N^+$, 60), 188 ($C_{13}H_{18}N^+$, 32), 185 ($C_{13}H_{15}N^+$, 28), 175 ($C_{12}H_{17}N^+$, 54), 150 ($C_{10}H_{16}N^+$, 44), 141 ($C_{11}H_9^+$, 87), 112 (Fe_2^+, 84), 97 ($C_6H_{11}N^+$, 17), 83 ($C_6H_{11}^+$, 15), 56 (Fe^+, 100), 41 ($C_3H_5^+$, 13); IR (CH_2Cl_2, 298 K) [cm^{-1}] 2061 (m), 2024 (vs), 1981 (s, br), 1964 (sh); ^1H NMR ($CDCl_3$, 298 K) [ppm] 1.01−1.87 (m, 10H, CH_2), 2.19−2.26 (m, 1H, CH), 4.20 (s, 2H, CH_2), 7.26 (d, $^3J_{HH} = 8.9$ Hz, 1H, CH), 7.50−7.58 (m, 2H, CH), 7.68−7.76 (m, 1H, CH), 7.87−7.96 (m, 2H, CH); ^{13}C NMR ($CDCl_3$, 298 K) [ppm] 26.1 (CH_2), 26.2 (CH_2), 35.4 (CH_2), 62.3 (CH), 74.1 (CH_2), 107.6 (C), 124.8 (CH), 125.7 (CH), 127.4 (CH), 127.5 (CH), 129.2 (CH), 133.5 (C), 134.2 (C), 142.7 (CH), 153.8 (C), 210.5 (CO). Anal. Calcd for $C_{23}H_{19}NO_6Fe_2$: C, 53.42; H, 3.70; N, 2.71. Found: C, 53.33; H, 3.93; N, 2.77.

MS and Spectroscopical Data of 2: MS (EI) *m/z* (%) 511 (M^+, 12), 483 ($M^+ - CO$, 8), 455 ($M^+ - 2$ CO, 27), 427 ($M^+ - 3$ CO, 8), 399 ($M^+ - 4$ CO, 28), 371 ($M^+ - 5$ CO, 67), 343 ($M^+ - 6$ CO, 100), 287 ($C_{17}H_{13}NFe^+$, 61), 260 ($C_{15}H_{10}NFe^+$, 9), 230 ($C_{17}H_{12}N^+$, 14), 215 ($C_{16}H_9N^+$, 21), 202 ($C_{15}H_8N^+$, 21), 183 ($C_{13}H_{13}N^+$, 19), 171 ($C_{12}H_{13}N^+$, 69), 139 ($C_{11}H_7^+$, 12), 112 (Fe_2^+, 14), 77 ($C_6H_5^+$, 7), 56 (Fe^+, 38); IR (CH_2Cl_2, 298 K) [cm^{-1}] 2066 (m), 2030 (vs), 1989 (s, br), 1974 (sh); ^1H NMR ($CDCl_3$, 298 K) [ppm] 4.68 (s, 2H, CH_2), 7.04−7.14 (m, 3H, CH), 7.20−7.34 (m, 3H, CH), 7.48−7.60 (m, 2H, CH), 7.74−7.79 (m, 1H, CH), 7.83−7.92 (m, 2H, CH); ^{13}C NMR ($CDCl_3$, 298 K) [ppm] 73.6 (CH_2), 105.5 (C), 122.8 (CH), 124.6 (CH), 125.6 (CH), 126.1 (CH), 127.4 (CH), 127.6 (CH), 129.0 (CH), 129.2 (CH), 133.4 (C), 134.8 (C), 142.5 (CH), 156.2 (C), 158.8, (C), 210.1 (CO). Anal. Calcd for $C_{23}H_{23}NO_6Fe_2$: C, 54.06; H, 2.56; N, 2.74. Found: C, 54.09; H, 2.64; N, 2.88.

MS and Spectroscopical Data of 3: MS (EI) *m/z* (%) 511 (M^+, 12), 483 ($M^+ - CO$, 9), 455 ($M^+ - 2$ CO, 10), 427 ($M^+ - 3$ CO, 12), 399 ($M^+ - 4$ CO, 29), 371 ($M^+ - 5$ CO, 35), 343 ($M^+ - 6$ CO, 52), 287 ($C_{17}H_{13}NFe^+$, 23), 230 ($C_{17}H_{12}N^+$, 86), 216 ($C_{16}H_{10}N^+$, 17), 202 ($C_{15}H_8N^+$, 22), 171 ($C_{12}H_{13}N^+$, 24), 167 ($C_{12}H_9N^+$, 44), 149 ($C_{11}H_3N^+$, 100), 128 ($C_9H_6N^+$, 25), 112 (Fe_2^+, 31), 83 ($C_5H_9N^+$, 24), 77 ($C_6H_5^+$, 30), 71 ($C_4H_9N^+$, 57), 57 (FeH^+, 88), 56 (Fe^+, 63) 43 ($C_3H_7^+$, 55); IR (CH_2Cl_2, 298 K) [cm^{-1}] 2062 (m), 2019 (vs), 1983 (s, br), 1958 (sh); ^1H NMR ($CDCl_3$, 298 K) [ppm] 4.20 (s, 1H, CH), 5.26 (s, 1H, NH), 6.53−6.56 (m, 1H, CH), 6.87−7.03 (m, 3H, CH), 7.48−7.64 (m, 4H, CH), 7.72−7.92 (m, 2H, CH), 8.23−8.32 (m, 1H, CH); ^{13}C NMR ($CDCl_3$, 298 K) [ppm] 61.9 (CH), 68.5 (C), 100.6 (C), 117.7 (CH), 122.5 (CH), 125.5 (CH), 125.9 (CH), 127.5 (CH), 128.8 (CH), 129.5 (CH), 133.1 (C), 134.5 (C), 142.4 (CH), 152.0 (CH), 157.8, (C), 212.8 (CO). Anal. Calcd for $C_{23}H_{23}NO_6Fe_2$: C, 54.06; H, 2.56; N, 2.74. Found: C, 54.06; H, 2.54; N, 3.09.

MS and Spectroscopical Data of 4: MS (EI) *m/z* (%) 724 ($M^+ - Fe - 7$ CO, 2), 696 ($M^+ - Fe - 8$ CO, 2), 668 ($M^+ - Fe - 9CO$, 2), 640 ($M^+ - Fe - 10$ CO, 19), 584 ($M^+ - 2$ Fe − 10 CO, 4), 558 ($C_{32}H_{34}N_2Fe_2^+$, 13), 530 ($C_{28}H_{30}N_2Fe_2^+$, 4), 515 ($C_{29}H_{27}N_2Fe_2^+$, 15), 488 ($C_{17}H_{18}NFe_2(CO)_5^+$, 14), 460 ($C_{17}H_{18}NFe_2(CO)_4^+$, 30), 432 ($C_{17}H_{18}NFe_2(CO)_3^+$, 35), 404 ($C_{17}H_{18}NFe_2(CO)_2^+$, 74), 376 ($C_{17}H_{18}NFe_2(CO)^+$, 2), 348 ($C_{17}H_{18}NFe_2^+$, 3), 265 ($C_{11}H_7NFe_2^+$, 4), 237 ($C_{17}H_{19}N^+$, 39), 201 ($C_{11}H_7N_2Fe^+$, 5), 196 ($C_{14}H_{14}N^+$, 23), 182 ($C_{13}H_{12}N^+$, 15), 168 ($C_{12}H_{10}N^+$, 31), 154 ($C_{11}H_8N^+$, 49), 140 ($C_{10}H_6N^+$, 18), 128 ($C_9H_6N^+$, 29), 112 ($Fe_2^+$, 29), 84 ($C_6H_{12}^+$, 100), 56 ($Fe^+$, 94), 43 ($C_3H_7^+$, 15); IR ($CH_2Cl_2$, 298 K) [$cm^{-1}$]: 2058 (m), 2047 (vs), 1985 (vs, br), 1770 (m); ^1H NMR ($CDCl_3$, 298 K) [ppm] 0.98−1.82 (m, 20H, CH_2), 3.12−3.35 (m, 2H, CH), 6.72−7.95 (m, 14H, CH); ^{13}C NMR (toluene-d_8, 298 K) [ppm] 25.8 (CH_2), 25.9 (CH_2), 26.8 (CH_2), 26.9 (CH_2), 30.3 (CH_2), 35.5 (CH_2), 40.3 (CH_2), 71.1 (CH), 71.4 (CH), 116.1 (C), 124.4 (CH), 125.4 (CH), 127.0 (CH), 129.7 (C), 130.2 (CH), 133.8 (CH), 136.9 (CH), 140.0 (CH), 144.1 (C), 163.8 (C), no signals of CO ligands have been observed. Anal. Calcd for $C_{44}H_{34}N_2O_{10}Fe_4$: C, 54.25; H, 3.52; N, 2.88. Found: C, 55.08; H, 3.76; N, 2.51.

Treatment of β-Naphthylcarbaldimines with $Fe_2(CO)_9$. A 500 mg sample of $Fe_2(CO)_9$ (1.37 mmol) is reacted with 1.64 mmol of the respective β-naphthylcarbaldimine (R = C_6H_{11}, 380 mg; R = C_6H_5, 370 mg) in 30 mL of *n*-heptane at 50 °C. After 1 h all of the starting material is dissolved and the color of the solution has changed from light yellow to deep red. The volatile material is evaporated in vacuo, and the oily residue is dissolved in 10 mL of CH_2Cl_2. A 2 g portion of silanized silica gel is added, and the solvent is removed in vacuo. The product mixture is chromatographed on silica gel using mixtures of light petroleum (bp 40−60 °C) and CH_2Cl_2. In both reactions at first a small amount of $Fe_3(CO)_{12}$ is eluted. In the reaction of the β-naphthylcarbaldimine with R = C_6H_{11} 200 mg (28%) of **5** is obtained using pure light as the eluent, with a mixture of light petroleum/CH_2Cl_2 (10:1) 150 mg (17%) of **8** is observed, and the use of a mixture of light petroleum/CH_2Cl_2 (3:1) leads to the isolation of 144 mg (20%) of **7**. Using the β-naphthylcarbaldimine with R = C_6H_5 320 mg (46%) of **6** is obtained with a mixture of light petroleum/CH_2Cl_2 (10:1), the use of a mixture of light petroleum/CH_2Cl_2 (5:1) leads to the isolation of 40 mg (4%) of **9**, and increasing the ratio to 3:1 25 mg (5%) of **10** are collected. **5** and **6** both are of purple color, **7** is of red-brown color, and **8** and **9** both are orange colored, as is **10**. All compounds are recrystallized from mixtures of light petroleum/CH_2Cl_2 at −20 °C.

MS and Spectroscopical Data of 5: MS (EI) *m/z* (%) 517 (M^+, 5), 489 ($M^+ - CO$, 1), 461 ($M^+ - 2$ CO, 26), 433 ($M^+ - 3$ CO, 11), 405 ($M^+ - 4$ CO, 26), 377 ($M^+ - 5$ CO, 65), 349 ($M^+ - 6$ CO, 100), 293 ($C_{17}H_{19}NFe^+$, 3), 287 ($C_{17}H_{13}NFe^+$, 25), 265 ($C_{15}H_{14}NFe^+$, 17), 198 ($C_{14}H_{16}N^+$, 24), 188 ($C_{13}H_{18}N^+$, 21), 141 ($C_{11}H_9^+$, 24), 112 (Fe_2^+, 20), 97 ($C_6H_{11}N^+$, 5), 56 (Fe^+, 17); IR (CH_2Cl_2, 298 K) [cm^{-1}] 2058 (m), 2020 (vs), 1976 (s, br); ^1H NMR ($CDCl_3$, 298 K) [ppm] 0.84−2.15 (m, 10H, CH_2), 2.55−2.76 (m, 1H, CH), 4.30 (s, 2H, CH_2), 7.42−7.82 (m, 5H, CH), 8.74 (s, 1H, CH); ^{13}C NMR ($CDCl_3$, 298 K) [ppm] 26.2 (CH_2), 26.4 (CH_2), 35.9 (CH_2), 64.8 (CH), 76.0 (CH_2), 110.6 (C), 120.2 (CH), 126.4 (CH), 127.8 (CH), 128.4 (CH), 129.2 (C), 132.7 (C), 136.2 (C), 145.3 (CH), 159.9 (CH), 210.4 (CO). Anal. Calcd for $C_{23}H_{19}NO_6Fe_2$: C, 53.42; H, 3.70; N, 2.71. Found: C, 53.75; H, 4.08; N, 2.74.

MS and Spectroscopical Data of 6: MS (EI) *m/z* (%) 511 (M^+, 6), 483 ($M^+ - CO$, 5), 455 ($M^+ - 2$ CO, 31), 427 ($M^+ - 3$ CO, 10), 399 ($M^+ - 4$ CO, 25), 371 ($M^+ - 5$ CO, 45), 343 ($M^+ - 6$ CO, 100), 315 ($M^+ - 5CO - Fe$, 2), 287 ($C_{17}H_{13}NFe^+$, 68), 260 ($C_{15}H_{10}NFe^+$, 7), 230 ($C_{17}H_{12}N^+$, 19), 215 ($C_{16}H_9N^+$, 11), 202 ($C_{15}H_8N^+$, 18), 182 ($C_{13}H_{12}N^+$, 12), 171 ($C_{12}H_{13}N^+$, 49), 139 ($C_{11}H_7^+$, 11), 112 (Fe_2^+, 13), 77 ($C_6H_5^+$, 9), 56 (Fe^+, 33); IR (CH_2Cl_2, 298 K) [cm^{-1}] 2064 (m), 2025 (vs), 1984 (s, br); ^1H NMR ($CDCl_3$, 298 K) [ppm] 4.66 (s, 2H, CH_2), 7.18−7.85 (m, 10H, CH), 8.72 (s, 1H, CH); ^{13}C NMR ($CDCl_3$, 298 K) [ppm] 76.0 (CH_2), 109.5 (C), 122.7 (CH), 124.4 (CH), 125.6 (CH), 126.8 (CH), 127.5 (CH), 127.9 (CH), 129.0 (CH), 131.9 (C), 133.7 (CH), 135.5 (C), 137.2 (C), 157.3 (CH), 159.8 (C), 210.3 (CO). Anal. Calcd for $C_{23}H_{23}NO_6Fe_2$: C, 54.06; H, 2.56; N, 2.74. Found: C, 54.40; H, 2.71; N, 2.74.

MS and Spectroscopical Data of 7: MS (EI) *m/z* (%) 517 (M^+, 2), 489 ($M^+ - CO$, 5), 461 ($M^+ - 2$ CO, 8), 433 ($M^+ - 4$ CO, 7), 377 ($M^+ - 5$ CO, 8), 349 ($M^+ - 6$ CO, 14), 321 ($M^+ - 5CO - Fe$, 13), 265 ($C_{15}H_{15}NFe^+$, 18), 237 ($C_{17}H_{15}N^+$, 76), 208 ($C_{15}H_{14}N^+$, 48), 194 ($C_{14}H_{12}N^+$, 69), 180 ($C_{13}H_{10}N^+$, 33), 166 ($C_{12}H_8N^+$, 30), 154 ($C_{11}H_8N^+$, 78), 141 ($C_{10}H_7N^+$, 86), 128 ($C_9H_6N^+$, 63), 112 (Fe_2^+, 51), 84 ($C_6H_{12}^+$, 100), 56 (Fe^+, 86), 41 ($C_3H_5^+$, 22); IR (CH_2Cl_2, 298 K) [cm^{-1}] 2061 (m), 2048 (s), 2020 (vs), 1991 (sh), 1977 (vs, br); ^1H NMR ($CDCl_3$, 298 K) [ppm]

1.12−2.08 (m, 10H), 3.07 (d, $^2J_{HH}$ = 21.3 Hz, 1H, part of a AB-pattern of the diastereotopic protons at C9), 3.10−3.25 (m, 1H, CH), 3.42 (d, $^2J_{HH}$ = 21.3 Hz, 1H, part of a AB-pattern of the diastereotopic protons at C9), 5.90 (s, 1H, CH), 6.90−7.27 (m, 4H, CH), 8.17 (s, 1H, N═CH); ^{13}C NMR (CDCl$_3$, 298 K) [ppm] 25.4 (CH$_2$), 25.7 (CH$_2$), 25.8 (CH$_2$), 31.8 (CH$_2$), 34.0 (CH$_2$), 34.7 (CH$_2$), 70.0 (CH), 81.6 (C), 88.0 (C), 125.0 (CH), 126.0 (CH), 126.6 (CH), 128.6 (CH), 130.4 (CH), 141.3 (C), 179.0 (N═CH), 194.9 (CO). Anal. Calcd for $C_{23}H_{19}NO_6Fe_2$: C, 53.42; H, 3.70; N, 2.71. Found: C, 52.26; H, 3.96; N, 2.85.

MS and Spectroscopical Data of 8: MS (EI) *m/z* (%) 657 (M$^+$, 1), 629 (M$^+$ − CO, 16), 601 (M$^+$ − 2 CO, 1), 573 (M$^+$ − 3 CO, 31), 545 (M$^+$ − 4 CO, 36), 517 (M$^+$ − 5 CO, M$^+$ − 3 CO − Fe, 43), 489 (M$^+$ − 6 CO, M$^+$ − 4 CO − Fe, 100), 451 (M$^+$ − 7 CO, M$^+$ − 5 CO − Fe, 72), 433 (M$^+$ − 8 CO, M$^+$ − 6 CO − Fe, 73), 405 (M$^+$ − 9 CO, M$^+$ − 7 CO − Fe, 100), 377 (M$^+$ − 8 CO − Fe, M$^+$ − 6 CO − Fe, 58), 349 (M$^+$ − 9 CO − Fe, M$^+$ − 7 CO − Fe, 84), 321 (M$^+$ − 8 CO − 2 Fe, 293), 293 (M$^+$ − 8 CO − 2 Fe, 30), 265 (M$^+$ − 9 CO − 3 Fe, 51), 201 ($C_{14}H_{19}N^+$, 91), 196 ($C_{14}H_{14}N^+$, 49), 182 ($C_{13}H_{12}N^+$, 49), 167 ($C_{12}H_9N^+$, 38), 154 ($C_{11}H_8N^+$, 28), 141 ($C_{10}H_7N^+$, 47), 112 (Fe_2^+, 38), 84 ($C_6H_{12}^+$, 78), 56 Fe$^+$, 39); IR (CH$_2$Cl$_2$, 298 K) [ppm] 2060 (m), 2048 (s), 2019 (s), 1976 (vs, br); ^{1}H NMR (CDCl$_3$, 298 K) [ppm] 0.95−1.90 (m, 10H, CH$_2$), 2.05−2.28 (m, 1H, CH), 3.50 (dd, $^3J_{HH}$ = 5.8 Hz, $^4J_{HH}$ = 1.9 Hz, 1H, CH), 3.51 (d, $^2J_{HH}$ = 11.8 Hz, 1H, part of a AB-pattern of the diastereotopic protons at C11), 3.62 (dd, $^3J_{HH}$ = 5.8 Hz, $^4J_{HH}$ = 1.9 Hz, 1H, CH), 3.75 (d, $^2J_{HH}$ = 11.8 Hz, 1H, part of a AB-pattern of the diastereotopic protons at C11), 6.26−6.37 (m, 2H, CH), 6.58 (s, 1H, CH), 7.21 (s, 1H, CH); ^{13}C NMR (CDCl$_3$, 298 K) [ppm] 25.9 (CH$_2$), 26.0 (CH$_2$), 26.3 (CH$_2$), 35.1 (CH$_2$), 35.8 (CH$_2$), 62.1 (CH), 62.4 (CH), 64.7 (CH), 74.0 (CH$_2$), 86.6 (CH), 86.9 (CH), 117.6 (CH), 124.9 (C), 138.8 (C), 140.0 (CH), 140.6 (C), 146.5 (C), 208.3 (CO), 210.7 (CO), 211.0 (CO). Anal. Calcd for $C_{26}H_{19}NO_9Fe_3$ C, 47.53; H, 2.91; N, 2.13. Found: C, 47.72; H, 3.03; N, 1.98.

MS and Spectroscopical Data of 9: MS (EI) *m/z* (%) 651 (M$^+$, 1), 623 M$^+$ − CO, 3), 595 (M$^+$ − 2 CO, 2), 567 (M$^+$ − 3 CO, 10), 539 (M$^+$ − 4 CO, 6), 511 (M$^+$ − 5 CO, M$^+$ − 3 CO − Fe, 8), 483 (M$^+$ − 6 CO, M$^+$ − 4 CO − Fe, 40), 455 (M$^+$ − 7 CO, M$^+$ − 5 CO − Fe, 37), 427 (M$^+$ − 8 CO, M$^+$ − 6 CO − Fe, 27), 399 (M$^+$ − 9 CO, M$^+$ − 7 CO − Fe, 44), 371 (M$^+$ − 8 CO − Fe, M$^+$ − 6 CO − 2 Fe, 25), 343 (M$^+$ − 9 CO − Fe, M$^+$ − 7 CO − 2 Fe, 87), 287 (M$^+$ − 9 CO − 2 Fe, 100), 230 ($C_{17}H_{12}N^+$, 55), 199 ($C_{10}H_9NFe^+$, 42), 171 ($C_8H_5NFe^+$, 36), 141 ($C_{10}H_9N^+$, 22), 112 (Fe_2^+, 27), 84 ($C_5H_{10}N^+$, 45), 56 (Fe$^+$, 56), 43 ($C_3H_7^+$, 11); IR (CH$_2$Cl$_2$, 298 K) [cm^{-1}] 2064 (m), 2050 (s), 2023 (vs), 1984 (vs, br); ^{1}H NMR (CDCl$_3$, 253 K) [ppm] 3.55 (d, $^3J_{HH}$ = 6.3 Hz, 1H, CH), 3.63 (d, $^3J_{HH}$ = 6.0 Hz, 1H, CH), 3.98 (d, $^2J_{HH}$ = 12.1 Hz, 1H, part of a AB-pattern of the diastereotopic protons at C11), 4.08 (d, $^2J_{HH}$ = 12.1 Hz, 1H, part of a AB-pattern of the diastereotopic protons at C11), 6.32−6.36 (m, 2H, CH), 6.69 (s, 1H, CH), 6.96−7.54 (m, 6H, CH); ^{13}C NMR (CDCl$_3$, 253 K) [ppm] 61.9 (CH), 62.0 (CH), 76.4 (CH$_2$), 86.7 (CH), 86.9 (CH), 118.5 (CH), 119.9 (C), 123.8 (CH), 128.6 (C), 128.8 (CH), 129.4 (CH), 139.3 (CH), 143.8 (C), 145.7 (C), 158.7 (C), 208.4 (CO), 210.3 (CO), 210.6 (CO). Anal. Calcd for $C_{26}H_{13}NO_9Fe_3$: C, 47.98; H, 2.01; N, 2.15. Found: C, 48.12; H, 2.09; N, 2.25.

MS and Spectroscopical Data of 10: MS (EI) *m/z* (%) 371 (M$^+$, 2), 343 (M$^+$ − CO, 8), 315 (M$^+$ − 2 CO, 20), 287 (M$^+$ − 3 CO, 82), 230 ($C_{17}H_{12}N^+$, 100), 202 ($C_{15}H_8N^+$, 11), 144 ($C_{10}H_{10}N^+$, 15), 115 ($C_8H_5N^+$, 12), 77 ($C_6H_5^+$, 24), 56 (Fe$^+$, 19); IR (CH$_2$Cl$_2$, 298 K) [cm^{-1}] 2064 (vs), 2021 (vs), 1989 (vs, br), 1967 (sh); ^{1}H NMR (CDCl$_3$, 253 K) [ppm] 5.29 (s, 1H, CH), 6.50 (d, $^3J_{HH}$ = 7.7 Hz, 1H, CH), 6.61 (d, $^3J_{HH}$ = 7.7 Hz, 1H, CH), 6.7−7.8 (m, 10H, CH); ^{13}C NMR (CDCl$_3$, 253 K) [ppm] 53.6 (CH), 89.6 (C), 113.6 (CH), 120.5 (CH), 121.1 (CH), 124.9 (CH), 126.1 (CH), 126.2 (CH), 127.4 (CH), 127.7 (CH), 128.1 (CH), 128.9 (CH), 129.1 (CH), 129.3 (CH), 136.9 (C), 137.6 (C), 146.6 (C), 208.2 (CO), 209.1 (CO). Anal. Calcd for $C_{20}H_{13}NO_3Fe$: C, 64.72; H, 3.53; N, 3.77. Found: C, 64.23; H, 3.61; N, 3.58.

Acknowledgment. The author gratefully thanks the Deutsche Forschungsgemeinschaft (SFB 436) for financial support.

Supporting Information Available: Details about the X-ray crystal structures including ORTEP diagrams of the crystal packings, tables of crystal data and structure refinement, atomic coordinates, bond lengths and angles, and anisotropic displacement parameters for **1**−**10**. This material is available free of charge via the Internet at http://pubs.acs.org.

OM990067Z